International Journal of Mass Spectrometry and Ion Processes, 88 (1989) 319–332
Elsevier Science Publishers B.V., Amsterdam – Printed in The Netherlands

OPEN-ENDCAP PENNING TRAPS FOR HIGH PRECISION EXPERIMENTS

G. GABRIELSE, L. HAARSMA and S.L. ROLSTON *

Department of Physics, Harvard University, Cambridge, MA 02138 (U.S.A.)

(Received 29 September 1988)

ABSTRACT

Cylindrical Penning traps with open-endcap electrodes are compared with the hyperbolic traps which are currently used for high precision experiments. Cylindrical traps are easier to construct and allow free access to the center of the trap for particle loading, laser beams, or microwaves. The trapping potential can be tuned while particles are inside the trap to improve harmonicity. Special geometries are noted which allow anharmonicities to be tuned out without affecting the trap well depth, and the effects of trap imperfections and gaps between the electrodes are discussed. Such traps will be used for measuring the antiproton mass, for cooling of trapped antiprotons, and possibly for producing antihydrogen.

INTRODUCTION

Penning traps are used to hold a single charged particle or a cloud of charged particles in a small volume. The simplest Penning trap consists of a strong magnetic field, which provides radial confinement, and an electric field which prevents particles from escaping along the magnetic field lines. If particle containment is the only goal, neither the shape of the electrodes used to apply the electric field nor the homogeneity of the magnetic field is especially important (except that a good symmetry under rotation about the magnetic field axis is required for long containment times [1]).

Penning traps have been used for high precision studies in which the trap and the trapped particles are treated as a bound system. Examples include precise measurements of the magnetic moments of the electron and the positron [2], the proton-to-electron mass ratio [3] and studies of relativistic electron motion at millielectronvolt energies [4]. The Penning traps used in these experiments had electrodes shaped like hyperboloids of revolution

* Present address: National Institute of Standards and Technology, Gaithersburg, MD 20899, U.S.A.

0168-1176/89/$03.50

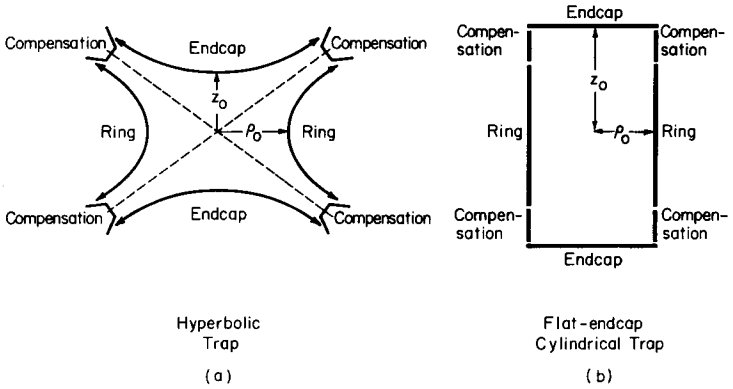

Fig. 1. Compensated Penning trap designs used in high precision measurements, with conventions for dimensions and potentials applied.

(Fig. 1a) because this geometry most nearly produces a quadrupole electric potential at the center of the trap. Such a potential is harmonic along the magnetic field axis and the particles oscillate between the trap endcaps with a frequency which is very insensitive to the oscillation amplitude. High precision measurements of this and other frequencies can be carried out when unavoidable misalignments and imperfections in trap electrodes are detected using particles inside the trap and are tuned out. An extra set of compensation electrodes is introduced for this purpose [5], and the electrostatics of this process are theoretically understood [6,7]. With an appropriate geometry, the trapping well depth can be made independent of anharmonicity tuning, to make an "orthogonalized" Penning trap [6].

A Penning trap with a cylindrical ring electrode and flat endcaps (Fig. 1b) has also been studied to determine its appropriateness for precision measurements. An orthogonalized geometry was identified [8] and then used to obtain a narrow axial resonance line width of a cloud of electrons [9]. Very recently a single electron was also observed in this trap [10]. Cylindrical Penning traps have two important advantages. First, cylindrical electrodes can be machined to greater accuracy in much less time than hyperbolic electrodes. Second, it is easier to study theoretically the anharmonicity compensation for a cylindrical trap than for hyperbolic shapes because the potentials can be calculated analytically.

Cylindrical Penning traps with long, open-ended endcap electrodes have already been used to produce polarized electron beams [11] and to trap antiprotons for up to 10 min [12]. The great advantage of this electrode configuration is the open access to the interior of the trap, which makes it easy to load particles and to introduce microwaves or laser beams. In this paper we study the addition of compensation electrodes to the open-endcap

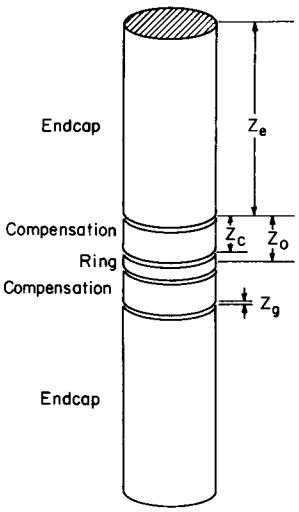

Fig. 2. Open-endcap Penning trap.

cylindrical trap to make this configuration more suitable for precision work without restricting the open access to the center of the trap. We identify a geometry for which anharmonicity compensation can be carried out without changing the axial well depth and use, as an example (Fig. 2), a trap which is intended for use in measuring the antiproton mass [13].

Other configurations of electrodes have been studied recently but, since anharmonicity compensation was not included, they are not suitable for the types of measurements mentioned above [14,15]. We use the notation of a recent review of the theory of a particle in a Penning trap [16].

POLYNOMIAL EXPANSION OF THE ELECTRIC POTENTIAL

The electric potential V near the center of a Penning trap can be expanded in Legendre polynomials in the usual way

$$V = \tfrac{1}{2} V_0 \sum_{\substack{k=0 \\ \text{even}}}^{\infty} C_k \left(\frac{r}{d}\right)^k P_k(\cos\theta) \tag{1}$$

where V_0 is the trapping potential, and the characteristic distance

$$d^2 = \tfrac{1}{2}\left(z_0^2 + \tfrac{1}{2}\rho_0^2\right) \tag{2}$$

is chosen because of its usefulness in hyperbolic traps, which we are trying to approximate. The Legendre polynomials $P_k(\cos\theta)$ are used because

azimuthal symmetry is maintained. Only the even k coefficients C_k will be non-zero when reflection symmetry across the $z = 0$ plane is assumed.

The lowest order terms in Eq. 1 are the most important for a particle trapped near the center of the trap. C_0 is an overall constant and can be ignored. In a perfect quadrupole potential (which is approximated by a hyperbolic trap), $C_2 = 1$ and all other terms equal zero. The frequency of axial oscillations ω_z is given, to lowest order, by

$$\omega_z^2 = \frac{qV_0}{md^2} C_2 \tag{3}$$

for a particle with mass m and charge q.

When $C_4 \neq 0$, the axial oscillator is anharmonic, with the oscillation frequency depending on the amplitude. The shift in the axial frequency is [8]

$$\frac{\Delta\omega_z}{\omega_z} = \frac{3}{2}\left(\frac{C_4}{C_2}\right)\frac{E_z}{qV_0C_2} \tag{4}$$

where E_z is the energy in the particle's axial oscillation. The ratio E_z/qV_0C_2 is typically quite small, but not negligible during precision measurements. Cylindrical Penning traps will certainly have a non-zero C_4 term. Even hyperbolic Penning traps have $C_4 \neq 0$, owing to machining imperfections, misalignments, endcap truncation, and other factors. Because amplitude-dependent shifts in the axial frequency are highly undesirable when small shifts in ω_z are to be measured, compensation electrodes are introduced into all high precision Penning traps, including hyperbolic traps [6–8], to tune out C_4.

The second anharmonic term C_6 is less important than C_4 by a factor of $(r/d)^2$ for particles near the center of the trap. A non-zero C_6 causes shifts in ω_z proportional to the square of the oscillation amplitude. Its effect on the axial oscillation can be represented [8] as an effective amplitude-dependent $\tilde{C}_4$ by replacing C_4 in Eq. 4 with

$$\tilde{C}_4 = C_4 + \tfrac{5}{2} C_6 \frac{E_z}{qV_0C_2} \tag{5}$$

The cylindrical electrodes in Fig. 2 are symmetric under reflections across the $z = 0$ plane and under rotations about the z axis. If we apply a potential V_0 between the endcaps and the ring, and V_c to the compensation electrodes, the potential inside the trap can be written as the superposition

$$V = V_0\phi_0 + V_c\phi_c \tag{6}$$

where ϕ_0 and ϕ_c are solutions to Laplace's equation with the boundary

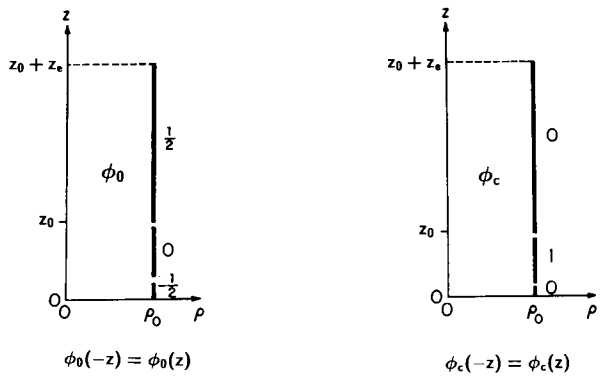

Fig. 3. Boundary conditions for solutions to Laplace's equations ϕ_0 and ϕ_c, both of which are invariant under rotations about the z axis and under reflections across the $z = 0$ plane.

conditions of Fig. 3. Near the center of the trap these solutions can be expanded as

$$\phi_0 = \tfrac{1}{2} \sum_{k=0}^{\infty} C_k^{(0)} \left(\frac{r}{d}\right)^k P_k(\cos\theta) \tag{7}$$

and

$$\phi_c = \tfrac{1}{2} \sum_{k=0}^{\infty} D_k \left(\frac{r}{d}\right)^k P_k(\cos\theta) \tag{8}$$

The C_k of Eq. 1 are then

$$C_k = C_k^{(0)} + D_k \frac{V_c}{V_0} \tag{9}$$

Lowest order anharmonicity compensation occurs when V_c is adjusted so that the two terms on the right cancel to make $C_4 = 0$.

The potentials ϕ_0 and ϕ_c are more naturally solved using a familiar expansion in Bessel functions of order zero.

$$V = V_0 \sum_{n=0}^{\infty} A_n J_0(ik_n\rho)\cos(k_n z) \tag{10}$$

where

$$k_n = \frac{(n + \frac{1}{2})\pi}{z_0 + z_e}. \tag{11}$$

and z_e is the length of the endcap electrodes. The Legendre polynomial coefficients C_k are determined by evaluating Eqs. 1 and 10 on the z axis and equating the coefficients of z^k. This yields for even k

$$C_k^{(0)} = \frac{(-1)^{k/2}}{k!} \frac{\pi^{k-1}}{2^{k-3}} \left(\frac{d}{z_0 + z_e}\right)^k \sum_{n=0}^{\infty} (2n+1)^{k-1} \frac{A_n^{(c)}}{J_0(ik_n\rho_0)} \tag{12}$$

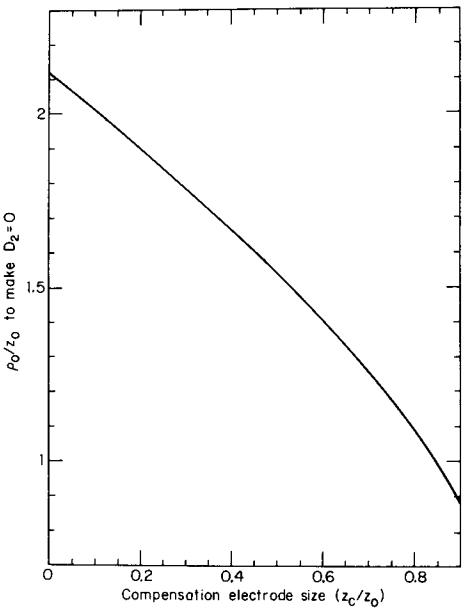

Fig. 4. Ratio ρ_0/z_0 required to orthogonalize the compensation electrodes.

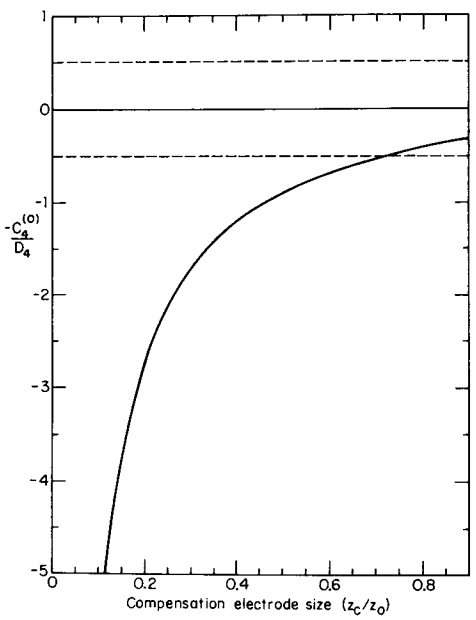

Fig. 5. Ratio V_c/V_0 required to make $C_4 = 0$ for an orthogonalized trap without imperfections. The broken lines at $+\frac{1}{2}$ and $-\frac{1}{2}$ represent the potentials on the endcap and ring electrodes, respectively.

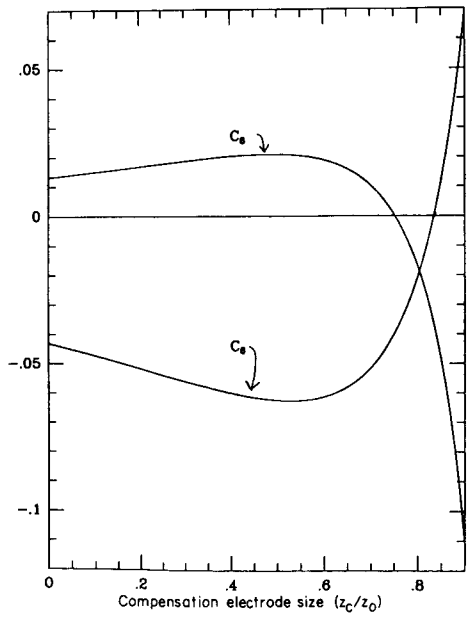

Fig. 6. Higher order coefficients when $C_4 = 0$.

and

$$D_k = \frac{(-1)^{k/2}}{k!}\frac{\pi^{k-1}}{2^{k-3}}\left(\frac{d}{z_0+z_e}\right)^k \sum_{n=0}^{\infty}(2n+1)^{k-1}\frac{A_n^{(d)}}{J_0(ik_n\rho_0)} \tag{12a}$$

with

$$A_n^{(c)} = \tfrac{1}{2}\{(-1)^n - \sin(k_n z_0) - \sin[k_n(z_0 - z_c)]\} \tag{13}$$

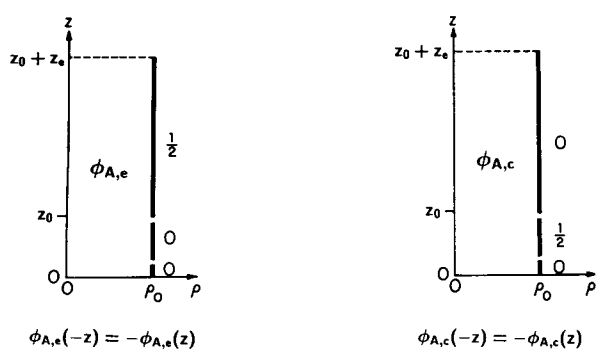

Fig. 7. Boundary conditions for $\phi_{A,e}$ and $\phi_{A,c}$ of Eqs. 15 and 16, both of which are symmetric under rotations about the z axis and antisymmetric under reflections across the $z = 0$ plane.

TABLE 1

Geometry and expansion coefficients of the open-endcap trap in Fig. 2

Electrode dimensions	
Radius (cm)	$\rho_0 = 0.600$
Length	$\rho_0/z_0 = 1.0239$
Compensation electrodes	$z_c/z_0 = 0.8351$
Endcap electrodes	$z_e/z_0 = 4.327$
Gaps between electrodes	$z_g/z_0 = 0.0303$
Axial frequency	
For electrons	$\nu_z = 9.63152 V_0^{1/2} (\mathrm{MHz}/V^{1/2})$
For protons	$\nu_z = 0.22477\ V_0^{1/2} (\mathrm{MHz}/V^{1/2})$

Expansion coefficients

$C_2^{(0)} = 0.5449$	$D_2 = 0$	$C_2 = 0.5449$	$c_1 = 0.3346$	$d_1 = 0.8994$
$C_4^{(0)} = -0.2119$	$D_4 = -0.5560$	$C_4 = 0$	$c_3 = 0.2202$	$d_3 = -0.8439$
$C_6^{(0)} = 0.1638$	$D_6 = 0.4300$	$C_6 = 0$	$c_5 = -0.0385$	$d_5 = 0.3915$
$C_8^{(0)} = -0.1359$	$D_8 = -0.2609$	$C_8 = -0.0365$	$c_7 = -0.0359$	$d_7 = -0.1251$

and

$$A_n^{(d)} = \sin(k_n z_0) - \sin[k_n(z_0 - z_c)]. \tag{13a}$$

Equations 12 and 13 assume that the endcap electrodes are infinitely long and that the gaps between the electrodes are negligibly small. These assump-

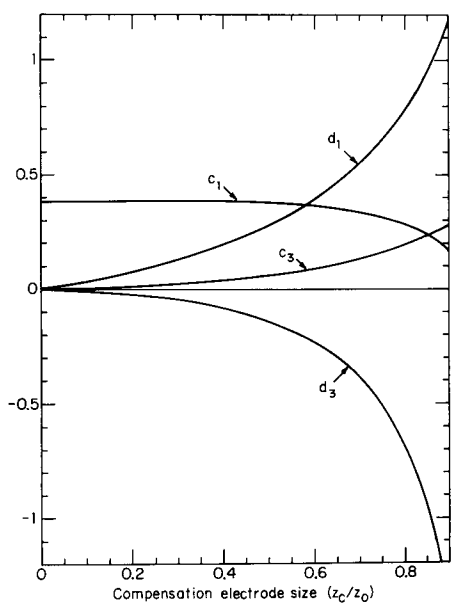

Fig. 8. Lowest order odd coefficients c_k and d_k.

TABLE 2

Effects of machining imperfections on the open-endcap trap in Fig. 2. Machining errors in the ratios of dimensions are expected to be of the order of one to ten parts in 1000

$$D_2 = 0 \quad -1.5\left(\frac{\Delta\rho_0}{z_0}\right) \quad -2.9\left(\frac{\Delta z_c}{z_0}\right) \quad -0.023\left(\frac{\Delta z_g}{z_0}\right)$$

$$C_6 = 0 \quad -0.33\left(\frac{\Delta\rho_0}{z_0}\right) +0.07\left(\frac{\Delta z_c}{z_0}\right) -0.007\left(\frac{\Delta z_g}{z_0}\right)$$

$$\left[\frac{V_c}{V_0}\right]_{C_4=0} = -0.3810 \quad -0.28\left(\frac{\Delta\rho_0}{z_0}\right) +0.44\left(\frac{\Delta z_c}{z_0}\right) +0 \quad \left(\frac{\Delta z_g}{z_0}\right)$$

$$\text{Proton} \quad \frac{\nu_z}{(V_0)^{1/2}} = 0.22477 \quad +0.023\left(\frac{\Delta\rho_0}{z_0}\right) -0.070\left(\frac{\Delta z_c}{z_0}\right) +0 \quad \left(\frac{\Delta z_g}{z_0}\right)$$

$$\text{Electron} \quad \frac{\nu_z}{(V_0)^{1/2}} = 9.63152 +1.0\left(\frac{\Delta\rho_0}{z_0}\right) -3.0\left(\frac{\Delta z_c}{z_0}\right) +0 \quad \left(\frac{\Delta z_g}{z_0}\right)$$

tions are not necessary for an exact solution. The effects of shortened endcaps and larger gaps can be included with slight modifications to Eqs. 12 and 13. It should be noted that these solutions converge when the endcap length is several times larger than its radius. (This can be proved analytically by solving the infinite endcap case with a Fourier integral and taking the limit in Eq. 10 as $z_e \to \infty$.) The coefficients C_k are already within 1% of the infinite endcap limit when $z_e/\rho_0 > 3$. In the rest of the paper we shall use the limit of long endcaps and negligible gaps (e.g. in Figs. 4–8) unless otherwise noted (e.g. Tables 1 and 2 and Fig. 9).

THE ORTHOGONALIZED TRAP

The coefficients $C_k^{(0)}$ and D_k are functions of the relative trap radius ρ_0/z_0 and compensation electrode size z_c/z_0. High precision measurements require that we make the anharmonic terms (C_4, C_6, etc.) as small as possible. From Eq. 9 we have seen that it is possible to make the leading C_4 contribution from the compensation electrodes cancel the C_4 contribution from the endcaps and ring by adjusting the compensation potential to

$$\left(\frac{V_c}{V_0}\right)_{C_4=0} = \frac{-C_4^{(0)}}{D_4} \tag{14}$$

Unfortunately, adjusting V_c to tune out C_4 generally changes C_2 and hence changes the axial resonance frequency ω_z. This is undesirable, since it requires a new search for the axial resonance every time an adjustment is made to V_c. However, if the trap is configured so that $D_2 = 0$, then, by Eq. 9,

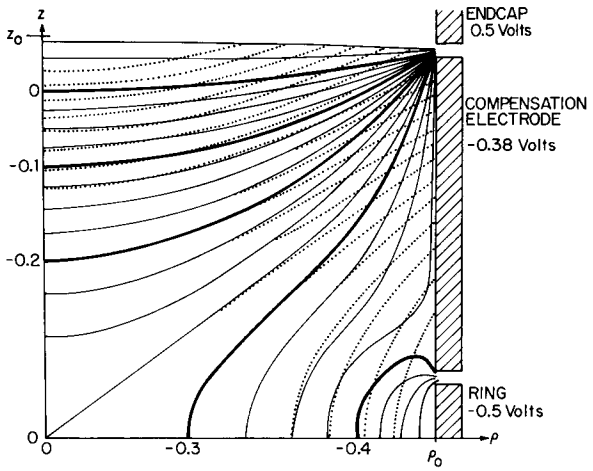

Fig. 9. Electrostatic field lines in the compensated, open-endcap trap of Fig. 2 and Tables 1 and 2 (solid) compared with field lines for a pure quadrupole potential (dotted).

adjusting V_c will have no effect on C_2. For any compensation electrode size z_c/z_0, there is a choice of trap radius ρ_0/z_0 such that $D_2 = 0$. This is called an "orthogonalized" Penning trap [8]. In an orthogonalized Penning trap, the axial frequency ω_z is independent of changes in V_c. The proper radius vs. compensation electrode size to produce an orthogonalized trap is shown graphically in Fig. 4. The compensation potential V_c/V_0 required to tune out C_4 in an orthogonalized trap with no imperfections, as a function of compensation electrode size, is shown in Fig. 5.

Since the trap can be orthogonalized for any compensation electrode size, we are free to pick any value for z_c/z_0 between 0 and 1. An interesting geometry is where C_6 equals zero, at $z_c/z_0 \approx 0.835$. At this point the compensation potential V_c/V_0 which makes $C_4 = 0$ simultaneously tunes out C_6. This could be very useful, since non-zero C_6 terms have noticeable effects in high precision measurements. In practice, we expect machining imperfections to give a non-zero $C_6 \approx 0.001$ (Table 2), but at least the contributions to C_6 from the trap geometry will be eliminated. We chose this geometry (Fig. 2) for the trap we intend to use in the antiproton mass measurement. Its geometry and expansion coefficients are shown in Table 1. As Fig. 9 shows, the electric potential in this trap resembles a pure quadrupole potential over a substantial region of the trap, with substantial departures from the center.

TRAP IMPERFECTIONS

Trap electrodes are never perfect. Patch effects, misalignments, and machining errors will change all of the $C_k^{(0)}$ and D_k from their calculated

values. One consequence is a slightly non-zero D_2, so that the trap is no longer properly orthogonalized. As Eq. 9 shows, a non-zero D_2 causes C_2 (and hence the resonant axial frequency ω_z) to change as V_c is adjusted. Also, D_4 will be modified slightly, but since D_4 is not nearly zero this is typically a small and insignificant change. More importantly, the imperfections will cause $C_4^{(0)}$ to shift from its calculated value. It will therefore be necessary to adjust V_c/V_0 while particles are inside the trap in order to tune out C_4. We can estimate how far $C_4^{(0)}$ might be from its calculated value by looking at some hyperbolic traps [6] which have already been built and used. A hyperbolic trap should have $C_4^{(0)} \approx 0$. Some existing traps (used for electron, positron, and proton work respectively) have $C_4^{(0)}$ of -4×10^{-3}, -2×10^{-3}, and 5×10^{-2}.

The effects of machining errors (specifically in the relative size of the radius, the length of the compensation electrode, and the gaps between the electrodes) have been carefully studied for the example trap of Fig. 2 and the results are given in Table 2. Machining errors in relative sizes should be of order one to ten parts in 1000.

Some well-compensated hyperbolic traps [6] have an amplitude-dependent anharmonicity $|\tilde{C}_4| < 10^{-4}$, once they are properly tuned. In order to achieve this with a cylindrical trap, it will be necessary to adjust and maintain V_c/V_0 to one part in 10^4. However, this is not difficult. It is especially important to keep the trapping potential V_0 as free from fluctuations as possible, since fluctuations in V_0 will directly effect ω_z. In an orthogonalized trap, ω_z is much more sensitive to fluctuations in V_0 than V_c because

$$D_2 = \frac{\partial \omega_z / \partial V_c}{\partial \omega_z / \partial V_0} \tag{15}$$

is so small.

DAMPING AND DRIVING AXIAL RESONANCE

There are several possible sources for an antisymmetric electric potential V_A in a Penning trap [7]. When a resistor is connected between the endcaps or between the compensation electrodes, the axial motion of the trapped particle itself will induce an antisymmetric potential. Radio frequency V_A might be deliberately applied to drive the axial resonance, or a small antisymmetric d.c. voltage V_{dc} might be deliberately applied to shift the center of axial oscillations. Solutions to Laplace's equation with the antisymmetric boundary conditions in Fig. 7 can be written as

$$\phi_{A,e} = \tfrac{1}{2} \sum_{k_{odd}=1}^{\infty} c_k \left(\frac{r}{z_0} \right)^k P_k(\cos \theta) \tag{16}$$

and

$$\phi_{A,c} = \tfrac{1}{2} \sum_{k_{\text{odd}}=1}^{\infty} d_k \left(\frac{r}{z_0} \right)^k P_k(\cos \theta) \tag{17}$$

for the endcap and compensation electrodes respectively.

A resistor R connecting the endcaps (or compensation electrodes) will damp the axial oscillations with a damping constant [7]

$$\Gamma_z = \frac{q^2}{m} \left(\frac{c_1}{2z_0} \right)^2 R \tag{18}$$

At the center of the trap, c_1 (or d_1) looks like a uniform electric field, and the equilibrium position of the particle is shifted from $z = 0$ to

$$z_{\text{equil.}} = \left(\frac{d^2}{2z_0} \right) \frac{c_1}{C_2} \left(\frac{V_{\text{dc}}}{V_0} \right) \tag{19}$$

It should be noted that an antisymmetric d.c. potential will shift the resonant axial frequency by an amount [16]

$$\frac{\Delta\omega_z}{\omega_z} = -\frac{3}{4} \left(\frac{d}{z_0} \right)^4 c_1 c_3 \left(\frac{V_{\text{dc}}}{V_0} \right)^2 \tag{20}$$

and can also cause an undesirable amplitude-dependent shift in the axial frequency. This sensitivity is best seen by extending Eq. 5 to read

$$\tilde{C}_4 = C_4 + \tfrac{5}{2} C_6 \frac{E_z}{m\omega_z^2 d^2} - \tfrac{5}{4} (c_3)^2 \left(\frac{V_{\text{dc}}}{V_0} \right)^2 \tag{21}$$

The leading coefficients, for the two boundary conditions in Fig. 7, are shown graphically in Fig. 8. It is desirable to have a large c_1 or d_1 in order to damp axial oscillations with a resistor, while a large c_3 or d_3 is a problem only if a large antisymmetric potential is applied. These can usually be kept quite small.

APPLICATIONS

Antiprotons have already been trapped for as long as 10 min in a simple open-endcap cylindrical trap [12]. Plans are currently under way to make a proton–antiproton mass comparison using the example trap shown in Fig. 2 and Tables 1 and 2. The open-endcap geometry is very important for this experiment. The trap is loaded when a pulse of antiprotons from a storage ring is sent into the trap through a slowing window which makes them spread radially, so that the large access hole is required. A second set of

endcap electrodes is placed beyond the first set and biased to high voltages (a few kilovolts) using a high speed switch [17] for the initial trapping of high energy antiprotons. As the antiprotons cool, they will eventually fall into the high precision part of the trap, where the mass measurement can be made after the outer endcaps are grounded.

Open-endcap traps could be useful for making antihydrogen [18]. A cloud of positrons can be trapped in the high precision region of the trap, between the inner set of endcaps. Then an outer set of endcaps can be negatively biased to capture antiprotons, creating a "nested trap" [9]. Trapped antiprotons will travel back and forth through the positron cloud, with some chance of capturing a positron on each pass.

CONCLUSION

Cylindrical Penning traps with open endcaps have several advantages over the hyperbolic traps currently used for high precision work. They allow free access to the center of the trap, making it easier to introduce particles into the trap. Cylindrically shaped electrodes are also much easier to machine.

Compensation electrodes can tune out anharmonicities and turn the open-endcap trap into a tool for high precision measurements. Orthogonalization of the compensation electrodes allows for the tuning out of anharmonicities without affecting the resonant axial frequency ω_z and reduces the sensitivity of the trap to fluctuations in the compensation voltage V_c. It is possible, with the right geometry, to tune out the first-order and reduce the second-order anharmonicities simultaneously. The geometry of this trap makes it ideal for use in experiments that require loading of particles from an external source. In addition, it allows for the construction of nested Penning traps, to combine clouds with charge of opposite sign.

ACKNOWLEDGEMENTS

This work was supported by the National Science Foundation, The National Bureau of Standards, and the Air Force Office of Scientific Research.

REFERENCES

1 J.H. Malmberg and T.M. O'Neil, Phys. Rev. Lett., 39 (1977) 1333.
2 R.S. Van Dyck, Jr., P.B. Schwinberg and H.G. Dehmelt, Phys. Rev. Lett., 59 (1987) 26.
3 R.S. Van Dyck, Jr., F.L. Moore, D.L. Farnham and P.B. Schwinberg, Int. J. Mass Spectrom. Ion Processes, 66 (1985) 327.
4 G. Gabrielse, H.G. Dehmelt and W. Kells, Phys. Rev. Lett., 54 (1985) 537.

5 R.S. Van Dyck, Jr., D.J. Wineland, P.A. Ekstrom and H.G. Dehmelt, Appl. Phys. Lett., 28 (1976) 446.
6 G. Gabrielse, Phys. Rev. A, 27 (1983) 2277.
7 G. Gabrielse, Phys. Rev. A, 29 (1984) 462.
8 G. Gabrielse and F.C. Mackintosh, Int. J. Mass Spectrom. Ion Processes, 57 (1984) 1.
9 G. Gabrielse, K. Helmerson, R. Tjoelker, X. Fei, T. Trainor, W. Kells and H. Kalinowsky, in L. Pinsky and B. Bonner (Eds.), Proc. Workshop on Low Energy Antiprotons, Fermilab, 1986.
10 J. Tan, C.H. Tseng and G. Gabrielse, Bull. Am. Phys. Soc., 33 (1988) 931.
11 J. Byrne and P.S. Farago, Proc. Phys. Soc. London, 86 (1965) 808.
12 G. Gabrielse, X. Fei, K. Helmerson, S.L. Rolston, R. Tjoelker, T.A. Trainor, H. Kalinowsky, J. Haas and W. Kells, Phys. Rev. Lett., 57 (1986) 2504.
13 G. Gabrielse, in P. Bloch, P. Paulopoulos and R. Klapisch (Eds.), Fundamental Symmetries, Plenum, New York, 1987.
14 E.C. Beaty, Phys. Rev. A, 33 (1986) 3645.
15 E.C. Beaty, J. Appl. Phys., 61 (1987) 2118.
16 L.S. Brown and G. Gabrielse, Rev. Mod. Phys., 58 (1986) 233.
17 X. Fei, R. Davisson and G. Gabrielse, Rev. Sci. Instrum., 58 (1987) 2197.
18 G. Gabrielse, L. Haarsma, S.L. Rolston and W. Kells, Phys. Lett. A, 129 (1988) 38.

Erratum:

Open-endcap Penning Traps for High Precision Experiments

[Int. J. of Mass Spectrom. and Ion Processes **88** (1989) 319-332.]

G. Gabrielse, L. Haarsma, S.L. Rolston

On page 330, a negative sign was omitted from Eq. (19)

$$z_{equil.} = \left(\frac{-d^2}{2z_0}\right)\frac{c_1}{C_2}\left(\frac{V_{DC}}{V_0}\right), \tag{19}$$

and factors of C_2 (required when C_2 differs from unity) were omitted from Eq. (20)

$$\frac{\Delta\omega_z}{\omega_z} = -\frac{3}{4}\left(\frac{d}{z_0}\right)^4\frac{c_1c_3}{C_2{}^2}\left(\frac{V_{DC}}{V_0}\right)^2 \tag{20}$$

and Eq. (21)

$$\tilde{C}_4 = C_4 + \tfrac{5}{7}C_6\frac{E_z}{m\omega_z^2d^2} - \frac{5}{4}\left(\frac{d}{z_0}\right)^6\frac{c_3{}^2}{C_2}\left(\frac{V_{DC}}{V_0}\right)^2. \tag{21}$$